Miscibility of Poly(butyl acrylate)−Poly(butyl methacrylate) Sequential Interpenetrating Polymer Networks

J. M. Meseguer Dueñas,[†] D. Torres Escuriola,[‡] G. Gallego Ferrer,[‡] M. Monleón Pradas,[‡] J. L. Gómez Ribelles,*[,‡] P. Pissis,[§] and A. Kyritsis[§]

Department of Applied Physics and Department of Applied Thermodynamics, Center for Biomaterials, Universidad Politécnica de Valencia, Camino de Vera s/n, E-46071 Valencia, Spain, and Department of Physics, National Technical University of Athens, Zografou Campus, 15780 Athens, Greece

Received November 30, 2000

ABSTRACT: The aim of this work is to study by means of dielectric and dynamic-mechanical techniques the miscibility and molecular mobility of sequential interpenetrating polymer networks (IPNs). Sequential poly(butyl acrylate)/poly(butyl methacrylate) interpenetrating networks with different cross-linking densities were prepared using ethylene glycol dimethacrylate as cross-linking agent. Loosely cross-linked IPNs undergo phase separation, as detected by the occurrence of two clearly differentiated main dielectric and dynamic-mechanical relaxation processes corresponding to the two components. Forced compatibilization phenomenon appears in the highly cross-linked IPNs. The IPN cross-linked with 10% EGDMA shows a single main dynamic-mechanical relaxation process. Only the α main relaxation process appears in the PBA networks within the temperature range of the experiments conducted in this work. The dielectric relaxation spectrum of PBMA networks shows the well-known β and α relaxation processes, which coalesce in a single $\alpha\beta$ relaxation in the merging region. In the compatibilized IPNs, both the α and the β relaxation shift toward lower temperatures as the amount of PBA segments in the IPN increases. The merging region shifts toward lower temperatures as well. In addition to these relaxation processes originated by the homogeneous mixture of PBA and PBMA segments, the IPNs containing more than 50% PBA also show the main PBA's dielectric relaxation process slightly shifted toward higher temperatures. This fact implies that an important part of the PBMA segments is mixed with PBA at the molecular level.

1. Introduction

Two polymeric materials in network form occupying the same spatial region form an interpenetrated polymer network (IPN). Swelling a polymer network of component A in the monomer of component B and then polymerizing the second network forms a sequential IPN. Most IPNs show phase separation. The physical laws that explain miscibility and phase separation in polymer blends also apply to IPNs; however, regarding phase separation some additional features have to be considered in the case of IPNs. Thus, a sequential IPN prepared with polymers that form compatible blends can present phase separation when the cross-linking density is small.[1] The phase morphology in sequential IPNs is affected by the miscibility of the polymer components, composition, cross-linking density, polymerization sequence (i.e., which polymer network is polymerized first as a pure network and which one is polymerized in the presence of the other component), and the kinetics of polymerization and phase separation.[2,3]

If polymers A and B are immiscible and the cross-linking density of A is small, i.e., the number of monomer units between cross-links is high, then during the polymerization of network B the growing B chains will push apart the already existing A chains, and a phase-separated IPN will be obtained. But if the cross-linking density of A is high, the positions of the A chains will hardly be changed, and the B network will grow interpenetrating the existing network A. Thus, a homogeneous IPN can eventually be obtained, achieving a forced compatibilization of both polymers.[4,5]

The occurrence of a single glass transition in a polymer blend or in an IPN is usually taken as proof of the homogeneity of the blend. Nevertheless, the temperature interval in which the glass transition takes place in a miscible blend is broader than in any of the pure components. Sometimes this temperature interval is extremely wide, reaching over 80 deg in blends such as polystyrene−poly(vinyl methyl ether).[6] This broadening of the glass transition has been connected to the existence of composition fluctuations in the material in nanometer dimensions (see refs 7−13 and references therein) called nanoheterogeneities. Since this is the order of magnitude of the length of cooperativity in the glass transition, different regions with sizes of tens of cubic nanometers would have different glass transition temperatures. The existence of a distribution of glass transition temperatures in the material explains the broadening of the material's glass transition temperature interval.

The origins of the main dielectric or dynamic-mechanical relaxation are also the cooperative conformational motions of the polymer chains, and a broadening of the spectrum of relaxation times is also found in miscible blends with respect to those of the pure polymer components.[7−10] Several models have been proposed to relate the shape of the dielectric relaxation spectrum to concentration fluctuations. Kumar et al.[9] have shown that the presence of nanoheterogeneities in a polymer blend whose components have glass transition temperatures well apart from each other produces two dif-

[†] Department of Applied Physics, Universidad Politécnica de Valencia.
[‡] Department of Applied Thermodynamics, Universidad Politécnica de Valencia.
[§] National Technical University of Athens.
* To whom correspondence should be addressed.

10.1021/ma002046i CCC: $20.00
Published on Web 06/26/2001

ferentiated main relaxation processes: one with the low-T_g component's characteristics and another one corresponding to the mean composition. This can be called a dynamic heterogeneity, and it is due to the fact that the length of cooperativity of the conformational motions responsible for the main relaxation processes is smaller the higher the difference between the temperature of the material and the glass transition temperature is. Thus, at any temperature above the calorimetric or dilatometric glass transition of the blend, the length of cooperativity of the low-T_g component is very small, and there are domains with sizes in this order of magnitude containing only chains of this component. On the contrary, the length of cooperativity for the high-T_g component is higher than the size of the larger regions containing only chains of this component, and as a consequence, the relaxation process occurs in rearranging regions with an average blend composition.

The effect of blending on the local motions that originate the secondary relaxation is not well understood. As far as we know, there is no literature related to this topic in the case of PBA or PBMA, but there is some information about the secondary β relaxation of poly(methyl methacrylate) (PMMA). This relaxation process appears at lower temperatures and with a lower apparent activation energy in miscible blends of PMMA with bisphenol A polycarbonate.[14] It is also clearly shifted toward lower temperatures in polyurethane−PMMA IPNs with respect to pure PMMA.[15] Nevertheless, in miscible blends of PMMA with poly(vinylidene fluoride) the β relaxation appears exactly in the same position as in pure PMMA.[16]

The aim of this work is to study the phenomenon of forced compatibility in poly(butyl acrylate)/poly(butyl methacrylate), PBA/PBMA, sequential IPNs by dielectric and dynamic-mechanical techniques and its effects on the local and conformational motions of the polymer chains.

2. Experimental Section

Sequential interpenetrating polymer networks (IPNs) were prepared by block polymerization using benzoin as photoinitiator. Two series of IPNs were prepared: one of them with a 0.1 wt % and the other one with a 10 wt % of ethylene glycol dimethacrylate (EGDMA) as cross-linking agent. The same amount of EGDMA was added in the polymerization of the two component networks. The poly(butyl acrylate) network was polymerized in first place. A half millimeter thick sheet was obtained. This sheet was immersed in a solution of butyl methacrylate monomer (BMA) and ethanol containing EGDMA in the same EGDMA/monomer ratio as the PBA network and the photoinitiator. The swollen sample was exposed to ultraviolet light to polymerize the poly(butyl methacrylate) network. Low molecular weight substances were extracted from the IPN by boiling it in ethanol for 24 h and then drying it in vacuo to a constant weight.

In those series with a 10% of EGDMA, this procedure allowed to synthesize a series of IPNs with a content of PBA ranging between a 32 and 81 wt % by varying the ratio of PBMA/ethanol in the second stage of the synthesis. The pure PBMA network cross-linked with 10% EGDMA was also prepared following the same routine as in the case of the PBA network.

When the first PBA network is cross-linked with 0.1% EGDMA, the amount of BMA that it is able to absorb in equilibrium is much greater than in the other series. As a consequence, the procedure described above yielded IPNs containing always more than 80% of PBMA network, even when the first network was swollen in BMA/ethanol mixtures with low monomer content. To cover a broad range of IPN compositions, the first PBA network was immersed in pure BMA monomer containing the appropriate amounts of EGDMA and benzoine for different periods of time. The swollen network was then sealed in an aluminum container and allowed to homogenize for 24 h. Then, the swollen sample was exposed to ultraviolet light to polymerize the poly(butyl methacrylate) network. This way a series of IPNs with PBA content ranging between 9 and 78 wt % were prepared. The pure PBMA network with 0.1% of EGDMA was synthesized following the same routine as the PBA network.

Table 1. Composition and Preparation Details of the Samples

	% weight fraction of EGDMA	% weight fraction of PBA network	procedure of polymerization of the second network
PBA01	0.1	100	
IPN78−01	0.1	78	*a*
IPN50−01	0.1	50	*a*
IPN14−01	0.1	14	*a*
PBMA01	0.1	0	
PBA10	10	100	
IPN81−10	10	81	*b*
IPN67−10	10	67	*b*
IPN56−10	10	56	*b*
IPN45−10	10	45	*b*
IPN32−10	10	32	*b*
PBMA10	10	0	

[a] The PBA network was immersed in BMA for different periods of time and allowed to equilibrate before polymerizing the BMA network. [b] The PBA network was immersed in a mixture of BMA and ethanol and allowed to equilibrate before polymerizing the BMA network.

The IPN samples will be named IPN*XX*−*YY*, *XX* indicating the weight percent of PBA network in the IPN and *YY* is 01 or 10 indicating 0.1% or 10% of EGDMA as cross-linking agent. PBA*YY* and PBMA*YY* will be used for the pure PBA and PBMA networks. Table 1 contains all the information related to the composition and preparation of the samples.

Dielectric relaxation spectroscopy (DRS) conducted on the samples of the series with 0.1% EGDMA was performed in a General Radio 1689M dielectric analyzer in a frequency range between 90 and 10^5 Hz, using a Novocontrol BDS1300 cell thermostatized between −160 and 200 °C within 0.1 °C. In the series with 10% EGDMA two different equipments were used: a Schlumberger frequency response analyzer FRA 1260 with a buffer amplifier of variable gain and a working frequency of 10^{-2}−10^6 Hz and a Hewlett-Packard 4284 A with a working frequency range of 20 to LCR meter in the frequency range between 20 and 10^6 Hz. The sample was sandwiched between nickel-coated stainless steel electrodes in an Ando SE-70 dielectric cell. The temperature of measurement was controlled to a 0.1 °C between −65 and 200 °C by means of an Ando type TO-19 thermostatic oven. For the measurements in the 10^6−10^9 Hz frequency range, a Hewlett-Packard impedance/material analyzer 4291 A integrated with a Tabai Espec temperature chamber SU-240-Y in the temperature range −35 to 130 °C was employed. The sample was sandwiched between gold-coated brass electrodes.

Dynamic-mechanical analysis (DMA) was carried out in a Seiko DMS210 instrument at frequencies of 0.1, 1, and 10 Hz.

3. Results

The dynamic-mechanical relaxation spectrum of PBMA networks shows a single maximum, which corresponds to the main relaxation, or α, process. The temperature of the maximum in the loss tangent, measured at 1 Hz, henceforth called $T_{\alpha DMA}$, increases with the content of cross-linking agent (70 °C in PBMA01 (Figure 1b) and 107 °C in PBMA10 (Figure 2b)). The secondary β relaxation process[17] appears as a shoulder covering a broad temperature interval between −50 and 40 °C. The secondary γ relaxation, due to local motions in the outer

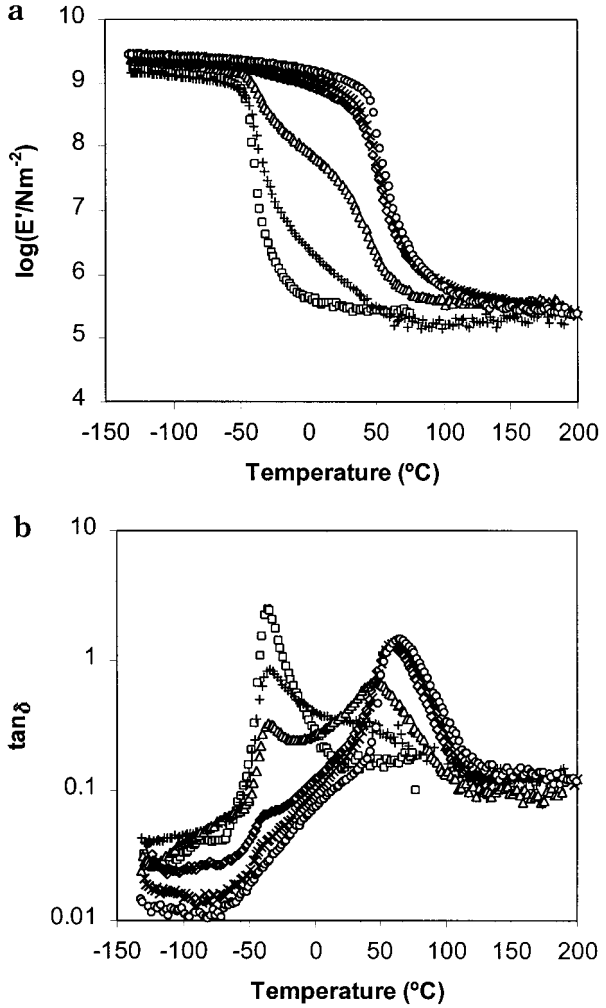

Figure 1. Temperature dependence of the elastic modulus (a) and the loss tangent (b) measured at 1 Hz in PBA01 network (□), IPN78−01 (+), IPN50−01 (△), IPN20−01 (◇), IPN09−01 (×), and PBMA01 network (○).

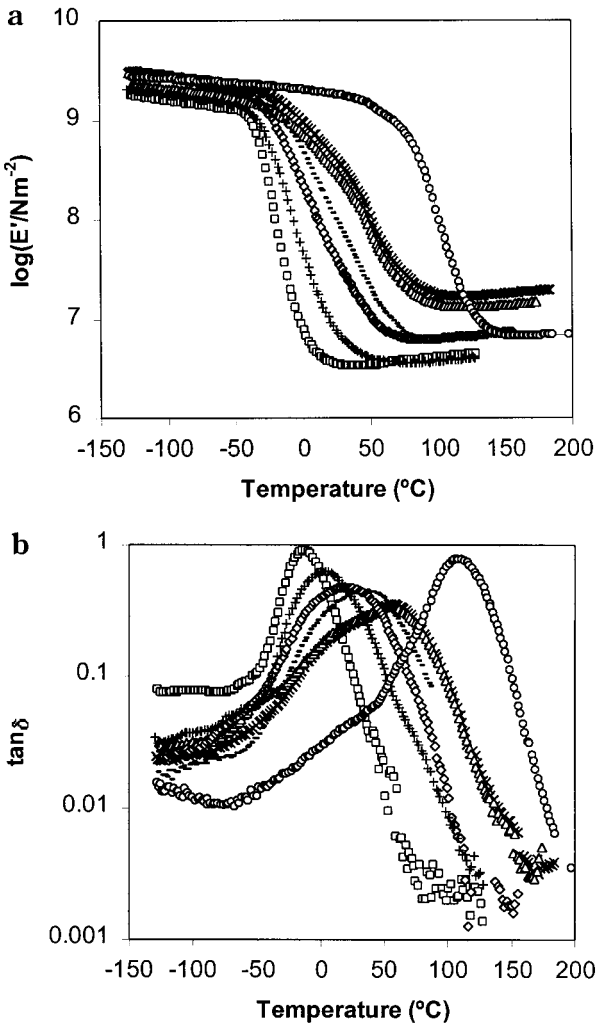

Figure 2. Temperature dependence of the elastic modulus (a) and the loss tangent (b) measured at 1 Hz in PBA10 network (□), IPN81−10 (+), IPN67−10 (◇), IPN56−10 (−), IPN45−10 (△), IPN32−10 (×), and PBMA10 network (○).

part of the side-chain group, would appear at lower temperatures than the temperature interval of our experiments.

Similar features can be observed in the case of the PBA network, but now the main relaxation process appears at −40 °C and −15 °C in the PBA01 (Figure 1b) and PBA10 (Figure 2b) networks, respectively, and the β relaxation appears as a very small peak in the loss tangent at around −85 °C.

The highly cross-linked IPNs show a single main relaxation process at a temperature ranging between those of the pure component networks (Figure 2). The broad peak of the loss tangent can be resolved into two overlapped peaks in the case of the IPNs with high PBMA content. The shoulder appearing in the low-temperature side of the maximum could correspond to the β relaxation of PBMA but could also be an indication of an incomplete merging of the main relaxation processes of the PBA and PBMA networks in the IPN.

On the other hand, the IPNs cross-linked with 0.1% EGDMA (Figure 1) show the main, α, relaxations of the PBA and PBMA networks clearly separated from each other. The temperature of the maximum in the loss tangent corresponding to the main relaxation of PBA network in the IPN slightly decreases as the PBA content in the IPN decreases. This behavior has been reported in other heterogeneous polymer systems, polymer blends, and polymer composites which consist of a continuous phase, or matrix, containing dispersed domains. In the mechanical experiments only the matrix material is clamped, and this makes a part of this component to work in series with the rest of the composite. The model simulation allows to explain the shift of the loss tangent peaks with no need of interface interaction (see refs 18 and 19 and the references there cited). These effects are less important in the case of dielectric spectroscopy.

The results of dielectric relaxation experiments are parallel to those of the dynamic mechanical spectroscopy. Figures 3 and 4 show the isochronous curves of the real and imaginary parts of the complex dielectric permittivity of the PBA and PBMA networks and the IPNs cross-linked with 10 and 0.1% EGDMA, respectively. The ϵ'' curves show the main, α, dielectric relaxations of PBA and PBMA networks merging into a single peak in the highly cross-linked IPNs, clearly revealing that it consists of two overlapped relaxation processes. The loosely cross-linked networks show two separated α peaks whose temperatures are slightly dependent on the composition of the IPN.

Dielectric relaxation spectroscopy allows a deeper insight into the characteristics of the relaxation processes due to the broad frequency range available for

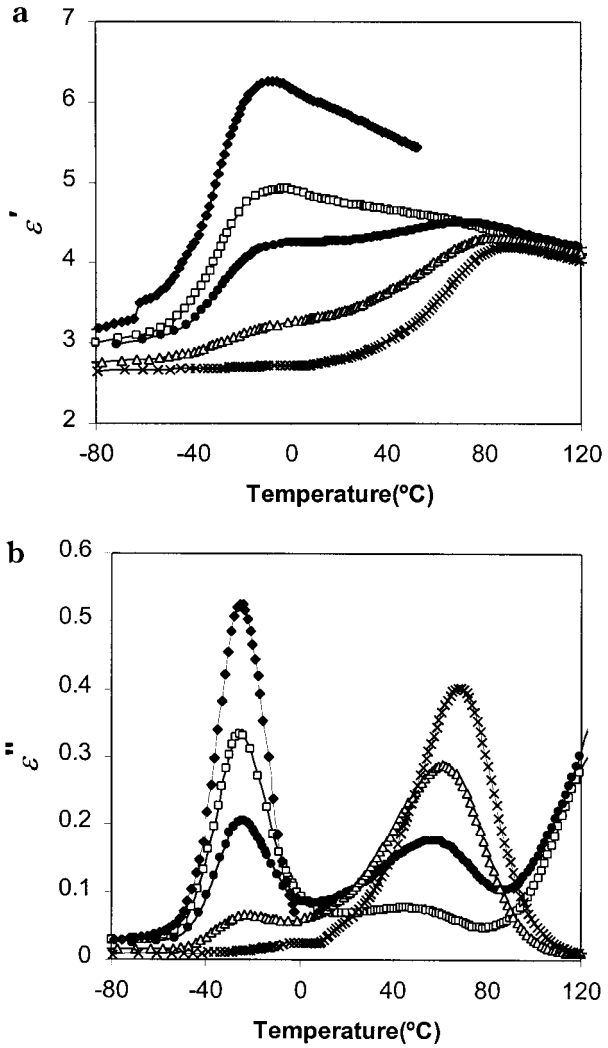

Figure 3. Temperature dependence of the complex dielectric permittivity: (a) ϵ' and (b) ϵ'' measured at 1 kHz in PBA01 network (◆), IPN78−01 (□), IPN50−01 (●), IPN14−01 (△), and PBMA01 network (×).

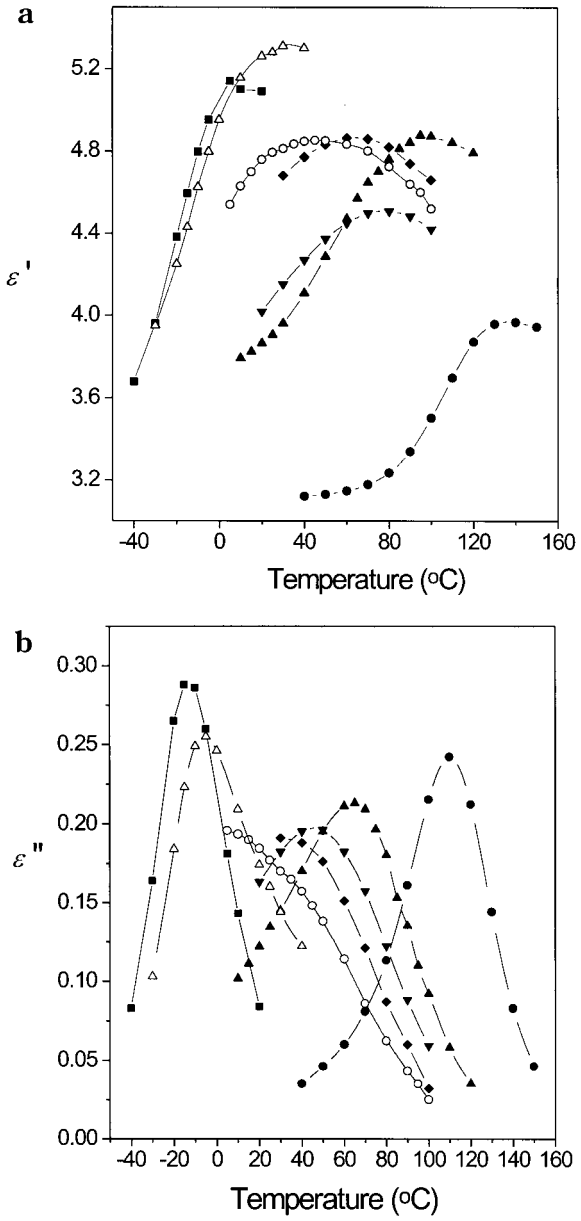

Figure 4. Temperature dependence of the complex dielectric permittivity: (a) ϵ' and (b) ϵ'' measured at 1 kHz in PBA10 network (■), IPN81−10 (△), IPN67−10 (○), IPN56−10 (◆), IPN45−10 (▼), IPN32−10 (▲), and PBMA10 network (●).

the experiments. In series IPN01, the α relaxation processes of the two networks are so far apart from each other that only one relaxation peak appears within the experimental frequency interval (results not shown) at any temperature. At low temperatures the peaks correspond to the α relaxation of PBA network, and at high temperatures they correspond to the α relaxation of PBMA network. The position of the maxima in the frequency axis is represented in the Arrhenius diagram of Figure 6a. While the position of the low-temperature relaxation in the IPNs exactly coincides with that of the main relaxation of PBA01 network, the high-temperature relaxation in the IPNs appears at higher frequencies (or lower temperatures) than the main relaxation of PBMA01 network. The temperature of this relaxation decreases as the PBA content of the IPN increases.

The behavior is different in the IPN10 series: for low PBA content the ϵ'' vs frequency isotherms show a single relaxation peak with a position in the frequency axis ranging between that of the main relaxations of PBA10 and PBMA10 networks. Figure 5b shows, as an example, the main relaxation of IPN10−45, and Figure 6b shows the position of the relaxation in the Arrhenius diagram. The IPNs containing 56 or 67% PBA show two relaxation peaks so close to each other that they are seen at the same temperature in the experimental frequency window. As an example of this behavior, Figure 5c shows the results obtained for the IPN10−67 sample. In these samples the relaxation times of the low-frequency peak follow an Arrhenius equation, as it happens in the IPNs with lower PBA content, while the high-frequency one shows a Vogel or Williams−Landel−Ferry (WLF) behavior similar to that of PBA10 network and also to IPN10−81, which shows a single relaxation peak.

Figure 5a shows the results obtained in PBA10 network. This relaxation process is thermorheologicaly simple with good approximation, and a master curve can be built, superposing the different isotherms, the same behavior found in un-cross-linked PBA.[20] This highly cross-linked network shows a broader α relaxation than the un-cross-linked polymer. The broadening of the main relaxation process with cross-linking is known from a long time ago; Mason[21] explained this

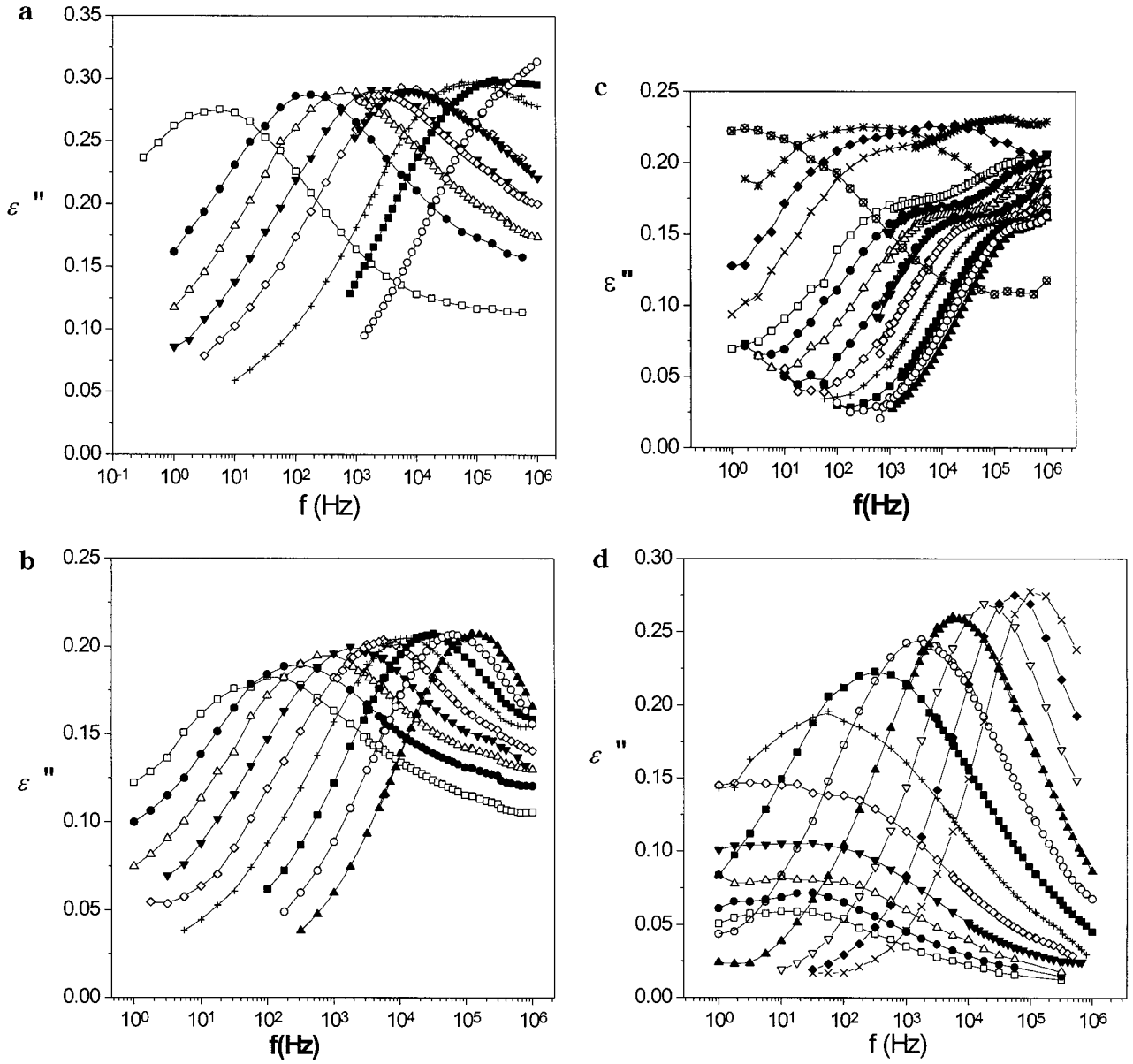

Figure 5. Frequency dependence of the imaginary part of the complex dielectric permittivity ϵ''. (a) PBA10 network: (□) −30 °C, (●) −20 °C, (△) −15 °C, (▼) −10 °C, (◇) −5 °C, (+) 5 °C, (■) 10 °C, (○) 20 °C. (b) IPN45−10: (□) 20 °C, (●) 30 °C, (△) 40 °C, (▼) 50 °C, (◇) 60 °C, (+) 70 °C, (■) 80 °C, (○) 90 °C, (▲) 100 °C. (c) IPN67−10: (⊗) −20 °C, (★) 0 °C, (◆) 10 °C, (×) 10 °C, (□) 30 °C, (●) 40 °C, (△) 50 °C, (▼) 60 °C, (◇) 70 °C, (+) 80 °C, (■) 90 °C, (○) 95 °C, (▲) 100 °C. (d) PBMA10 network: (□) 40 °C, (●) 50 °C, (△) 60 °C, (▼) 70 °C, (◇) 80 °C, (+) 90 °C, (■) 100 °C, (○) 110 °C, (▲) 120 °C, (▽) 130 °C, (◆) 140 °C, (×) 150 °C.

feature, in reference to the viscoelastic main relaxation, by the introduction of a distribution of monomeric free volume. Recently, it has been related to an increase of cooperativity with increasing cross-linking density.[22] The β relaxation in this network is small and appears at temperatures well below the α relaxation. Thus, the relaxation shown is nearly a pure α relaxation. This is also why the dependence of relaxation times follows the Vogel or WLF behavior. Nevertheless, in the PBMA10 network (Figure 5d), the β and α relaxations merge at frequencies close to the experimental ones;[23−26] this explains the change of the shape of the relaxation with increasing temperature. This means that the peak shown by the experimental ϵ'' curves is due to the overlapping of both relaxation processes. The contribution of each relaxation can be separated[26,27] by fitting the experimental curves to a model consisting of the sum of two Havriliak−Negami equations,

$$\epsilon^*(\omega) - \epsilon_\infty = \frac{\Delta\epsilon}{\left(1 + \left(i\frac{\omega}{\omega_0}\right)^b\right)^a} \qquad (1)$$

one for each overlapped relaxation. In eq 1 $f_0 = \omega_0/2\pi$ is the characteristic HN frequency, ϵ_∞ is the real component of the permittivity at high frequencies, and a and b are the shape parameters. When this fitting procedure is applied to the case of PBMA10 network, it is possible to determine the temperature dependence of the position in the frequency axis and the relaxation strength $\Delta\epsilon$ of each relaxation. The results of the fitting routine are similar to those found by Garwe et al. in PBMA[26] and Beiner et al. in poly(*n*-hexyl methacrylate).[27] At temperatures above 390 K the experimental ϵ'' vs frequency isotherms can be reproduced with a single Havriliak−Negami relaxation process which can be called $\alpha\beta$ process (it was called "*a*" process in refs 26 and 27). The intensity of the relaxation decreases with temperature

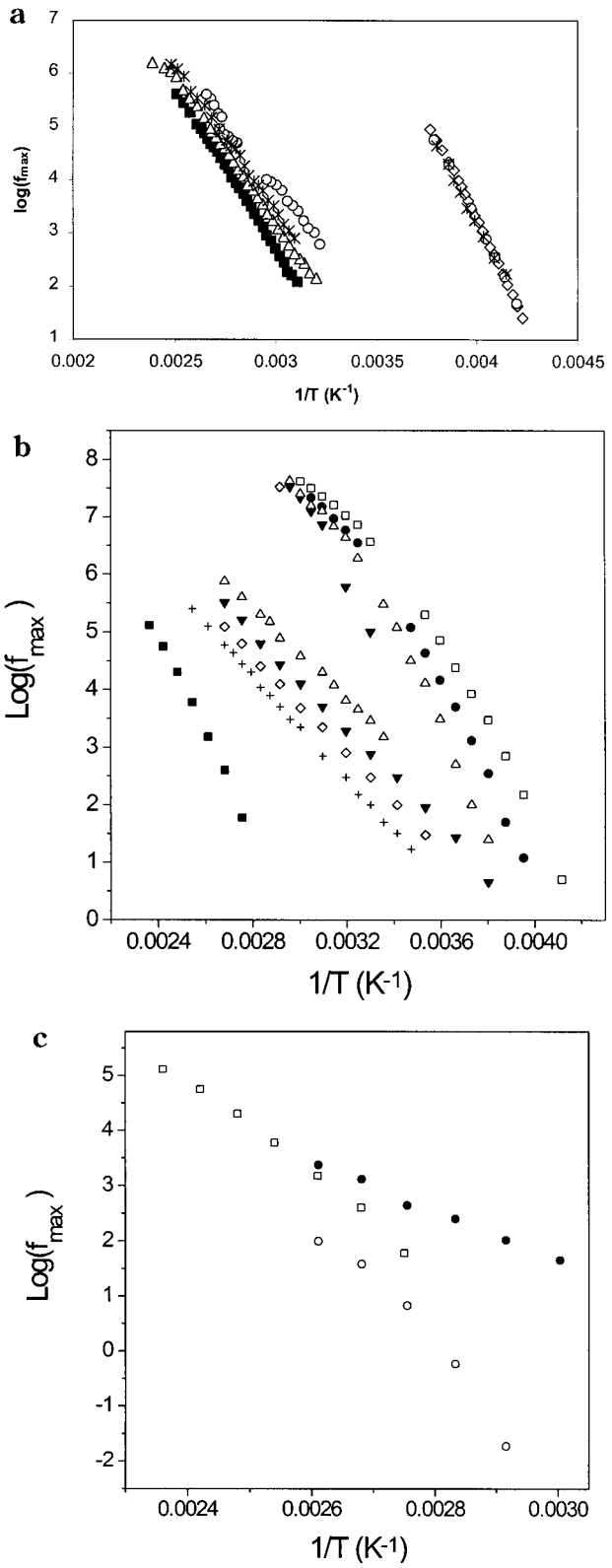

Figure 6. Arrhenius diagram showing the position of the relaxation processes of the series of networks cross-linked with 0.1% EGDMA (a) (PBA01 network (◇), IPN78−01 (△), IPN50−01 (∗), IPN14−01 (○), and PBMA01 network (■)) and with 10% EGDMA (b) PBA10 network (□), IPN81−10 (●), IPN67−10 (△), IPN56−10 (▼), IPN45−10 (◇), IPN32−10 (+) and PBMA10 network (■). Diagram (c) shows the position of the components α (○), β (●) of the relaxation spectrum of PBMA10 obtained by fitting the experimental curves to the sum of two Havriliak−Negami distributions (see text).

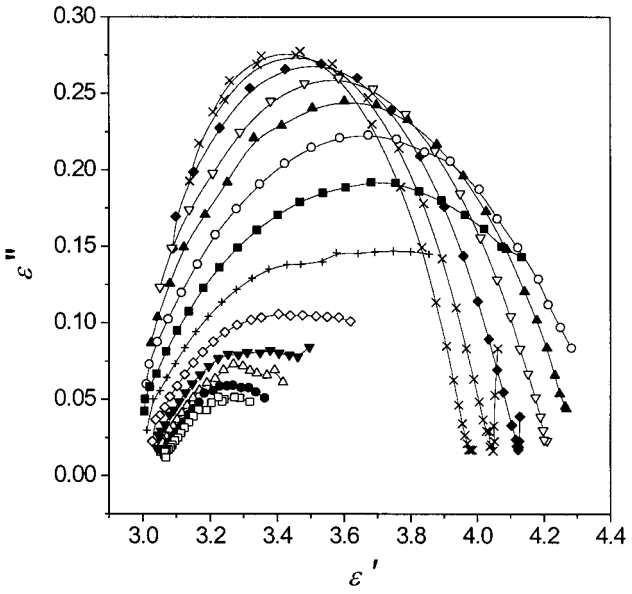

Figure 7. Cole−Cole diagrams of PBMA10 network: (□) 30 °C, (●) 40 °C, (△) 50 °C, (▼) 60 °C, (◇) 70 °C, (+) 80 °C, (■) 90 °C, (○) 100 °C, (▲) 110 °C, (▽) 120 °C, (◆) 130 °C, (×) 140 °C, (∗) 150 °C.

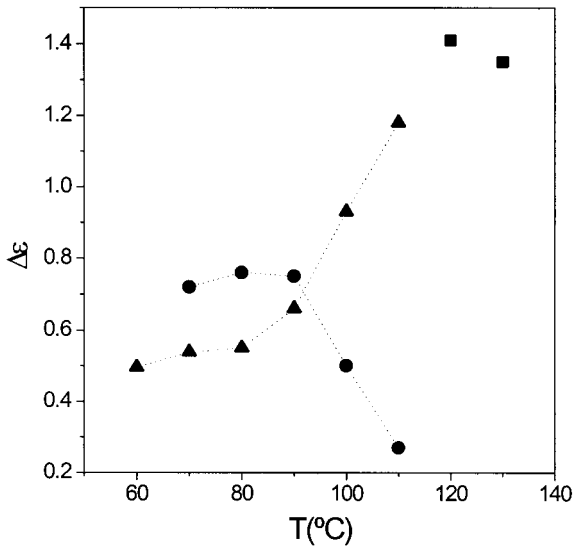

Figure 8. Relaxation strength of the components α (●) and β (▲) of the relaxation spectrum of PBMA10 obtained by fitting the experimental curves to the sum of two Havriliak−Negami distributions. Two points (■) corresponding to the αβ relaxation are also included (see text).

in this temperature region, as can be clearly seen, without recourse to curve fitting, in the ϵ' vs temperature plot of Figure 4 and in the Cole−Cole diagram of Figure 7, by a decrease of the limit of ϵ' at low frequencies when temperature increases above 110 °C. At temperatures below 120 °C, the contribution of the β relaxation is characterized by a relaxation strength value which increases with temperature, whereas the value of $\Delta\epsilon$ corresponding to the α contribution decreases with temperature tending to zero at around 120 °C (see Figure 8). This temperature can be called the onset of the α relaxation and is higher in the network than in PBMA homopolymer,[26] a behavior similar to that of the glass transition temperature.

In the overall relaxation spectrum, the temperature at which the strength of the relaxation goes through a maximum is an approximate indication of the transition

from the regime where two independent α and β relaxations coalesce to the αβ regime. This transformation can be determined by extrapolation in the Cole−Cole diagrams without having recourse to curve-fitting procedures. Figure 7 shows the Cole−Cole diagram of a series of isotherms measured in PBMA10. It can be observed that the limit of these isotherms at low values of ϵ' is nearly temperature independent, and the high value limit, corresponding to low frequencies, clearly decreases with increasing temperature above 100 °C.

The Arrhenius diagram of Figure 6c shows the trends of the high-frequency, i.e., β relaxation, and the low-frequency, i.e., α relaxation, the former showing an Arrhenius behavior with an apparent activation energy of 84 kJ/mol, close to the value determined in un-cross-linked PBMA,[28] and the latter showing WLF behavior. In Figure 6c the position of the maxima of ϵ'' vs frequency rough curves is also represented. It is clear that they are very close to those of the β relaxation which seems to be predominant in this representation. The representation of Figure 6c also allows to say that when $1/T$ is higher than approximately 0.0028 (i.e., temperature lower than 90 °C), the influence of the α relaxation on the experimental relaxation spectrum is very small since it occurs at very low frequencies. Thus, for these temperatures the experimental relaxation peak can be analyzed as a pure β relaxation. These results permit a study of the influence of the interpenetration with a PBA network on the local motions of PBMA network.

This procedure was not repeated in all IPNs, but the discussion of the former paragraphs allows one to say that the points shown in Figure 6b for the IPN10 samples with PBA contents less than or equal to 45% and the low-frequency peaks of IPN10−56 and IPN10−67 networks are a good approximation of the position of the β relaxation. This is especially true for the experimental points corresponding to the lowest temperatures in each network. The Cole−Cole arcs in the IPNs with 45% or less PBA show a pattern quite similar to that shown in Figure 7 for PBMA10. The transition from the α and β relaxations to the αβ regime (the temperature of the maximum in the strength of the overall relaxation) shifts to lower temperatures as the PBA content in the IPN increases. It takes place at 60−70 °C in the IPN containing 32% of PBA and at 30−40 °C in the IPN containing 45% of PBA. In samples with higher PBA content, the shapes of the Cole−Cole arcs are more complicated because of the overlapping of the two relaxation processes (results not shown).

4. Discussion

DMA and DRS results clearly show the forced compatibilization in PBA/PBMA IPNs. These results can be interpreted in terms of miscibility and phase separation of the IPN. To do that, it is necessary to distinguish between the static heterogeneity of an amorphous blend or IPN, i.e., the size of the domains of each component, and the dynamic heterogeneity revealed by the possibility of a cooperative conformational rearrangement taking place involving only polymer segments of one of the components. The dynamic heterogeneity is related to the occurrence of individual main dielectric and dynamic-mechanical relaxation processes and their characteristics.

The connection between static and dynamic heterogeneity can be explained with the aid of the Adam−Gibbs theory.[29] A cooperatively rearranging region (CRR) is a region of the material in which a conformational rearrangement can take place without disturbing the rest of the material. The volume of such a region, V_a, and the length of cooperativity associated with it (defined as $\lambda = V_a^{1/3}$) are highly dependent on temperature. The length of cooperativity is very small at high temperatures but increases with decreasing temperatures and at the glass transition temperature T_g it reaches values in the range of a few nanometers.[30,31] An heterogeneous blend or IPN consisting of a distribution of domains with compositions different from the average will be heterogeneous from the dynamic point of view at a temperature T, if the size of the domains with compositions different from the average are larger than the length of cooperativity corresponding to the temperature T and the composition of each domain. This means that a static heterogeneity in the scale of nanometers is enough to produce the dynamic heterogeneity, i.e., enough to be reflected by the relaxation behavior of the blend.

When the cross-linking density in PBA/PBMA IPNs is small, the IPN is heterogeneous enough to show two independent main relaxation processes. The main relaxation process of PBA appears exactly at the same temperature (Figure 6a) and with the same half-width (results not shown) as in the PBA01 network, which means that the conformational rearrangements occur in regions that contain only PBA chain segments. Nevertheless, the shift of the β dielectric relaxation of PBMA segments toward lower temperatures, as the PBA content in the IPN increases, is apparent. The high-temperature dynamic-mechanical relaxation shifts toward lower temperatures as the PBA content of the blend increases. The intensity of the dynamic-mechanical β relaxation is much smaller than that of the α relaxation. The evolution of the loss tangent peak with IPN concentration reflects the interaction between the IPN components as conformational rearrangements take place. Thus, every region in the nanometer scale contains some PBA chain segments blended with the PBMA network.

During the polymerization of the second network in the formation process of the sequential IPN the growing PBMA network pushes away the existing PBA chains, forming a separated PBMA phase, but the size of these domains is small enough to allow a dynamic interaction with the PBA chains.

The behavior of the highly cross-linked IPN10 series is much different from the IPN01 series. In the highly cross-linked IPN, a single maximum is detected in the temperature spectrum of the DMA loss tangent. The main DMA relaxation of both components merge into a single one, although the shoulder on the low-temperature side of the peak shown by the spectrum of the IPNs, which could be due to the β relaxation of PBMA, could also indicate that merging is not complete. Figure 9 shows the position of the maximum of the loss tangent as a function of the PBA content of the IPN. The composition dependence of T_α agrees with the Fox equation[32]

$$\frac{1}{T_\alpha} = \frac{w_{PBA}}{T_{\alpha,PBA}} + \frac{w_{PBMA}}{T_{\alpha,PBMA}}$$

where w_{PBA} and w_{PBMA} are the weight fractions of PBA and PBMA units in the IPN and $T_{\alpha,PBA}$ and $T_{\alpha,PBMA}$ are

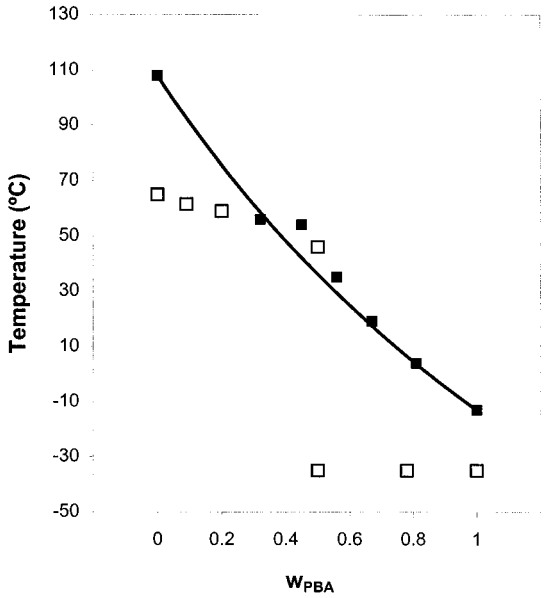

Figure 9. Composition dependence of the temperature of DMA (loss tangent measured at 1 Hz, squares) relaxation peaks of the IPN01 series (open symbols) and IPN10 series (full symbols).

the temperatures of the main α relaxation of the pure component networks.

The dielectric ϵ'' vs temperature plots also show a single maximum (Figure 4b). However, the analysis is not as easy as in the case of the dynamic-mechanical relaxation because the peak shown in the case of PBA network is due mainly to the α relaxation, but the one shown in the case of PBMA network corresponds to the superposition of the α and β mechanisms.

The difference between the behavior probed by DRS and by DMA lies in the different relative intensity of the β dielectric relaxation compared with the α one in the two techniques, due to the fact that the permanent dipolar moment resides in the side chain, and also in the different experimental frequencies scanned by each technique. In dielectric experiments, the relaxation spectrum is measured at temperatures well apart from the calorimetric or dilatometric glass transition temperature, T_g. At any temperature T the difference $T - T_g$ is around 70 deg greater for PBA domains than for PBMA, and as a consequence, the length of cooperativity at T is much smaller for a PBA network than for PBMA. The results obtained for IPN10−56 and IPN10−67 agree with the idea of Kumar et al.[9] The dielectric relaxation spectrum shows the relaxation process of the more mobile component (region I, at high frequencies) and, in addition, the relaxation processes corresponding to the average composition (region II at low frequencies). In the case of DMA experiments, the measurements are performed at 1 Hz, and thus the temperature is closer to T_g. The length of cooperativity is larger than in the dielectric response, and there is no clear separation of the α relaxation due to the species of the higher mobility.

In region I the experimental results show a shift toward higher temperatures in the high-frequency relaxation with respect to the PBA10 network. This means that no domains of pure PBA can be found even in the scales of the length of cooperativity corresponding to these high temperatures, which are of molecular dimensions.

Table 2. Dielectric Glass Transition Temperature (See Text) and the Parameters of Eq 2 for PBA and PBMA Networks and IPNs Cross-Linked with 0.1% of EGDMA

	log f_0	B	T_0	dielectric T_g
PBMA10				332
IPN67−10	13.29 ± 0.5	1795 ± 230	198 ± 6	247
IPN81−10	13.98 ± 0.5	2278 ± 220	176.4 ± 5	236
PBA10	13.2 ± 0.3	1969 ± 150	174.5 ± 4	228

The position of the main dielectric relaxation in the temperature axis can be characterized by the temperature at which the maximum of the α relaxation takes place at 10^{-3} Hz. This temperature can be called the dielectric T_g. The log f_{max} vs $1/T$ curves, showing the position of the maxima of ϵ'' vs f isotherms, were fitted to a Vogel equation

$$f_{max} = f_0 \exp\left(\frac{B}{T - T_0}\right) \quad (2)$$

The values of the fitting parameters are included in Table 2. In the case of PBMA10 network the data used was the position of the α relaxation obtained by curve fitting using the Havriliak−Nagami equation as explained in the preceding section. The value of the dielectric T_g was obtained by extrapolation of the experimental data without fitting since the frequency interval in which the data points were obtained is quite close to 10^{-3} Hz. The dielectric T_g for PBMA10, PBA10, and IPN81−10 and IPN67−10 are also included in Table 2. If one assumes that the shift in the glass transition is due to the dilution of the PBA network segments by some PBMA and that the composition dependence follows the Fox equation, similar to eq 1 for the dielectric T_g, then the observed values of the dielectric T_g allow to determine the amount of PBMA homogeneously diluted in the PBA phase. According to this, the phase responsible for the α dielectric relaxation observed in IPN81−01 contains a 90% of PBA whereas in IPN67−01 it contains a 76% of PBA. It can be said that around 50−60% of the PBMA participates in the α dielectric relaxation in these IPNs.

Region II corresponds to the superposition of the α and β relaxation mechanisms in PBMA 10 network. The dilution of some PBA segments in the PBMA makes the observed relaxation process shift toward lower temperatures, as shown in Figure 5 and in the Arrhenius diagram of Figure 6b. At low temperatures the observed relaxation is mainly due to the β mechanism, since the frequency of the α component is much lower, as discussed in the preceding section. Because of forced compatibilization, it is expected that the dielectric α mechanism will move toward low temperatures as the PBA content in the IPN increases, as in the dynamic-mechanical relaxation. The dielectric experimental results prove that the secondary relaxation accompanies the α relaxation. It has been shown in both polyacrylates and polymethacrylates that there is a close relationship between the strength of the α and β relaxations.[17,20,28,33] As the length of the side group increases in the PMMA−PEMA−PBMA series (or in PMA−PEA−PBA), the strength of the α relaxation increases while that of the β relaxation decreases. This was interpreted in the sense that the β relaxation is related to the residual mobility or the ability to reorient the permanent dipolar moment in the glassy state that is smaller as the length of the side group increases. As a consequence, the β relaxation always appears at a temperature below the α one and

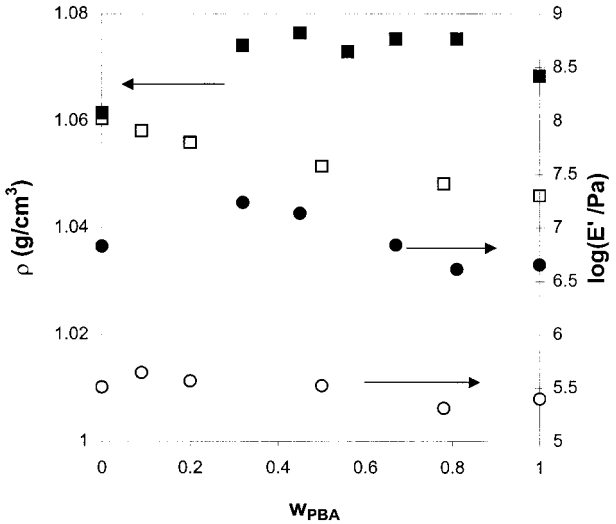

Figure 10. Density (squares) and elastic modulus at 130 °C of IPN01s (open symbols) and IPN10s (full symbols) as a function of the weight fraction of PBA in the IPN.

shifts toward lower temperatures in the IPNs as the α relaxation does. The merging of the α and β relaxation also shifts toward lower temperatures as the PBA content in the IPN increases. Although the temperature of the $\alpha\beta$ splitting region has not been determined accurately, there is an indication that the whole α and β relaxation process is influenced in a parallel way by the dilution of PBMA segments in the IPN by the presence of some PBA mixed with them.

Another strong indication of the miscibility of the two networks in the highly cross-linked IPNs is the value of the elastic modulus of the IPN in the rubber state. As shown in Figure 2a, E'_e is higher in some of the IPNs than in any of the PBA10 and PBMA10 pure networks. According to the theory of rubber elasticity, these values are closely related to the average molecular weight between cross-links, $\bar{M}_e$, according to

$$\bar{M}_e = \frac{\rho RT}{G_e} \qquad (3)$$

where G_e is the shear modulus in the elastomeric region which can be estimated as $G_e = E'_e/3$, ρ is the density, and R is the gas constant. Equation 3 is calculated using the affine network model.[34] Equation 3 was applied in the case of PBA networks, using the value of the density measured at 20 °C in rubberlike state and the value of the elastic modulus at the same temperature obtained by linear extrapolation to 20 °C of the experimental data in the rubberlike region (results shown in Figure 10), resulting in $\bar{M}_e = 31\,000$ g/mol in PBA01 and $M_e = 2300$ g/mol in PBA10.

In the case of PBMA networks and IPNs, the determination of the density in rubberlike state is not easy because the network is in glassy state around room temperature. Nevertheless, the differences in density between IPNs and pure PBMA10 and PBA10 networks are small compared with the differences in the elastic modulus (Figure 10). Thus, according to eq 3, the average length between cross-links or entanglements in the IPNs containing 32, 45, and 56% PBA and 10% EGDMA is smaller than in the pure networks. This feature has to be explained by the appearance of mutual entanglements between the two networks acting as new cross-links in the IPN.

5. Conclusions

Sequential PBA/PBMA IPNs cross-linked with 0.1% EGDMA are phase-separated, although some PBA segments are diluted in the PBMA-rich phase participating in its relaxation processes. The IPN can be compatibilized increasing the cross-linking density. The IPN cross-linked with 10% EGDMA shows a single main dynamic-mechanical relaxation process. Only the main, α, relaxation appears in the PBA networks in the temperature range of the experiments conducted in this work. The dielectric relaxation spectrum of PBMA networks shows the well-known β and α relaxation processes that coalesce into a single $\alpha\beta$ relaxation in the merging region. In the compatibilized IPNs, both α and β relaxation shift toward lower temperatures as the amount of PBA segments in the IPN increases. The merging region shifts toward lower temperatures as well. In addition to these relaxation processes which are due to the homogeneous mixture of PBA and PBMA segments, the IPNs containing more than 50% PBA also show the main dielectric relaxation process of the PBA, slightly shifted toward higher temperatures. This fact suggests that an important part of the PBMA segments are mixed with PBA at the molecular level.

Acknowledgment. J.M.M.D. acknowledges the support of the Generalitat Valenciana through project CV97-TI-06-36 and M.M.P. and J.L.G.R. the support of CICYT through the MAT97-0634-C02-01 project.

References and Notes

(1) Thomas, D. A.; Sperling, L. H. In *Polymer Blends*; Paul, D. R., Newman, S., Eds.; Academic Press: San Diego, 1978.
(2) Utracki, L. A. In *Interpenetrating Polymer Networks*; Klempner, D., Sperling, L. H., Utracki, L. A., Eds.; Advances in Chemistry Series; American Chemical Society: Washington, DC, 1994.
(3) Bauer, B. J.; Briber, M. In *Advances in Interpenetrating Polymer Networks;* Klempner, D., Frisch, K. C., Eds.; Technomic: Lancaster, 1994; Vol. 4.
(4) Li, B. Y.; Bi, X. P.; Zhang, D. H.; Wang, F. S. In *Advances in Interpenetrating Polymer Networks;* Klempner, D., Frisch, K. C., Eds.; Technomic: Lancaster, 1989; Vol. 1.
(5) Fradkin, D. G.; Foster, J. N.; Sperling, L. H.; Thomas, D. A. *Polym. Eng. Sci.* **1996**, *26*, 730.
(6) Cowie, J. M. G.; Ferguson, R.; Fernández, M. D.; Fernández, M. J.; McEwen, I. J. *Macromolecules* **1992**, *25*, 3170.
(7) Shears, M. S.; Williams, G. *J. Chem. Soc., Faraday Trans. 2* **1973**, *69*, 608.
(8) Wetton, R. E.; MacKnight, W. J.; Fried, J. R.; Karasz, F. E. *Macromolecules* **1978**, *11*, 158.
(9) Kumar, S. K.; Colby, R. H.; Anastasiadis, S. H.; Fytas, G. *J. Chem. Phys.* **1996**, *105*, 3777.
(10) Katana, G.; Fischer, E. W.; Hack, Th.; Abetz, V.; Kremer, F. *Macromolecules* **1995**, *28*, 2714.
(11) Roland, C. M.; Ngai, K. L. *Macromolecules* **1991**, *24*, 2261.
(12) Alvarez, F.; Alegría, A.; Colmenero, J. *Macromolecules* **1997**, *30*, 597.
(13) Chung, G. C.; Kornfield, J. A.; Smith, S. D. *Macromolecules* **1994**, *27*, 964.
(14) Landry, J. T. C.; Mark Henrichs, P. *Macromolecules* **1989**, *22*, 2157.
(15) Rizos, A. K.; Fytas, G.; Ma, R. J.; Wang, C. H.; Abetz, V.; Meyer, G. C. *Macromolecules* **1993**, *26*, 1869.
(16) Wing Sy, J.; Mijovic, J. *Macromolecules* **2000**, *33*, 933.
(17) McCrum, N. G.; Read, B. E.; Williams, G. *Anelastic and Dielectric Effects in Polymeric Solids;* Wiley: New York, 1967.
(18) Gómez Ribelles, J. L.; Monleón Pradas, M.; Más Estellés, J.; Meseguer Dueñas, J. M.; Romero Colomer, F. *Plastics Rubber Comp. Proc. Appl.* **1992**, *18*, 169.
(19) Gallego Ferrer, G.; Salmerón Sánchez, M.; Verdú Sánchez, E.; Romero Colomer, F.; Gómez Ribelles, J. L. *Polym. Int.* **2000**, *49*, 853.
(20) Gómez Ribelles, J. L.; Meseguer Dueñas, J. M.; Monleón Pradas, M. *J. Appl. Polym. Sci.* **1989**, *38*, 1145.

(21) Mason, P. *Polymer* **1964**, *5*, 625.
(22) Kramarenko, V. Y.; Ezquerra, T. A.; Šics, I.; Baltá-Calleja, F. J.; Privalko, V. P. *J. Chem. Phys.* **2000**, *113*, 447.
(23) Williams, G.; Edwards, D. A. *Trans. Faraday Soc.* **1966**, *62*, 1329.
(24) Williams, G. *Trans. Faraday Soc.* **1966**, *62*, 2091.
(25) Sasabe, H.; Saito, *J. Polym. Sci., Part A2* **1968**, *6*, 1401.
(26) Garwe, F.; Schönhals, A.; Lockwenz, H.; Beiner, M.; Schröter, K.; Donth, E. *Macromolecules* **1996**, *29*, 247.
(27) Beiner, M.; Kahle, S.; Hempel, E.; Schröter, K.; Donth, E. *Macromolecules* **1998**, *31*, 8973.
(28) Gómez Ribelles, J. L.; Díaz Calleja, R. *J. Polym. Sci., Polym. Phys. Ed.* **1985**, *23*, 1297.
(29) Adam, G.; Gibbs, J. H. *J. Chem. Phys.* **1965**, *43*, 139.
(30) Donth, E. *Relaxation and Thermodynamics in Polymers, Glass Transition*; Akademie Verlag: Berlin, 1992.
(31) Gómez Ribelles, J. L.; Vidaurre Garayo, A.; Cowie, J. M. G.; Ferguson, R.; Harris, S.; McEwen, I. J. *Polymer* **1998**, *40*, 183.
(32) Fox, T. G. *Bull. Am. Phys. Soc.* **1956**, *1*, 123.
(33) Heijboer, J. In *Physics of Non-Crystalline Solids*; Prins, J. A., Ed.; North-Holland: Amsterdam, 1965; p 231.
(34) Erman, B.; Mark, J. E. *Structure and Properties of Rubberlike Networks;* Oxford University Press: Oxford, 1997.

MA002046I